

## A Promising Beginning for Perovskite Nanocrystals: A *Nano Letters* Virtual Issue

The recent success of metal halide perovskites in solar cells has generated a frenzy of research centered on these once-overlooked semiconductors. A pair of key questions naturally arise: how will the nanocrystal version of these materials behave, and what can we do with them? Since the 1980s, the synthetic achievement of nanocrystals with defined shape, size, and surface chemistry has enabled new optoelectronic properties for a variety of applications, including displays, solar cells, photodetectors, single-photon sources, and fluorescence imaging.

As a hybrid of these two exciting research fields, perovskite nanocrystals are expected to exhibit some intriguing and unique properties. Indeed, they inherit many advantages of their perovskite parent materials: solution-phase processing, tunable band gaps, and tolerance to defects. This tolerance contributes to several attractive properties such as high photoluminescence quantum yields, high charge-carrier mobilities, and long carrier lifetimes. First-principles calculations<sup>1</sup> on halide perovskites indicate that the most common defects occur at energies near the band edges or within the bands; therefore, they do not act as deep traps.<sup>2</sup> This favorable electronic structure arises from the specific bonding energetics between the lead and halide atoms as well as spin–orbit coupling. However, as quantum dots, perovskite nanocrystals inherit the benefits of quantum confinement such as optoelectronic properties that are tunable with size and the emission of single photons. Furthermore, recent theoretical and experimental work shows that the lowest-energy exciton is an allowed, or so-called “bright,” transition, which is responsible for the rapid radiative recombination rates and extremely bright emission observed from perovskite nanocrystals.<sup>3</sup> Nevertheless, they also retain challenges such as lead toxicity, environmental instability and photoinstability, and difficulty with integration into macroscopic devices. Based on their remarkably varied compositional tunability,<sup>2</sup> however, they may offer new ways to overcome these obstacles. Whether they can ultimately outperform existing materials for specific applications or enable entirely new technologies remains to be seen. In this virtual issue, we highlight some of the recent progress and upcoming challenges in the field of halide perovskite nanocrystals, as featured in Table 1.

**Colloidal Synthesis and Post-synthetic Transformations.** The synthesis of perovskite nanocrystals has been inspired by the protocols used for conventional metal chalcogenide nanocrystals. In most approaches, metal cation and halide precursors are dissolved in a heated, noncoordinating organic solvent. Both acidic and basic ligands are used to improve solubility of the precursors and to prevent aggregation and precipitation of the nanocrystals. The ratios of these ligands, the temperature of the reaction, and the reaction time determine the size and shape of the resulting nanocrystals.<sup>4</sup> However, the kinetics of these reactions are faster than those seen in other quantum dot systems,<sup>5</sup> and the mechanisms of formation are only just beginning to be probed. New precursors to gain control over the reaction conditions are under active

**Table 1. References by Subject**

colloidal synthesis and post-synthetic transformations	
CH <sub>3</sub> NH <sub>3</sub> PbBr <sub>3</sub>	<i>J. Am. Chem. Soc.</i> , 2014, 136 (3), 850–853
CH <sub>3</sub> NH <sub>3</sub> PbX <sub>3</sub>	<i>ACS Nano</i> , 2015, 9 (4), 4533–4542
CsPbBr <sub>3</sub>	<i>ACS Nano</i> , 2016, 10 (8), 7943–7954
CsPbX <sub>3</sub>	<i>Nano Lett.</i> , 2015, 15 (6), 3692–3696; <i>J. Am. Chem. Soc.</i> , 2018, 140 (7), 2656–2664
CH(NH <sub>2</sub> ) <sub>2</sub> PbX <sub>3</sub>	<i>Nano Lett.</i> , 2017, 17 (5), 2765–2770
CsSnX <sub>3</sub>	<i>J. Am. Chem. Soc.</i> , 2016, 138 (9), 2941–2944
Cs <sub>2</sub> AgBiX <sub>6</sub>	<i>Nano Lett.</i> , 2018, 8 (2), 1118–1123
anion exchange	<i>Nano Lett.</i> , 2015, 15 (8), 5635–5640
cation exchange	<i>J. Am. Chem. Soc.</i> , 2017, 139, (11), 4087–4097
phase transformation	<i>Nano Lett.</i> , 2017, 17 (3), 1924–1930
doping with Mn <sup>2+</sup>	<i>J. Am. Chem. Soc.</i> , 2016, 138, (45), 14954–14961; <i>ACS Energy Lett.</i> , 2017, 2 (3), 537–543
beyond CsPbX <sub>3</sub>	<i>ACS Energy Lett.</i> , 2017, 2 (5), 1089–1098
bright, tunable emission and blinking dynamics	
absorption and emission	<i>Nano Lett.</i> , 2016, 16, (3), 1869–77; <i>Nano Lett.</i> , 2016, 16 (4), 2349–2362; <i>Nano Lett.</i> , 2015, 15 (6), 3692–3696; <i>Nano Lett.</i> , 2017, 17 (5), 2765–2770; <i>J. Am. Chem. Soc.</i> , 2016, 138 (9), 2941–2944
stimulated emission	<i>Nano Lett.</i> , 2016, 16 (1), 448–453; <i>J. Am. Chem. Soc.</i> , 138 (11), 3761–3768
photoluminescence blinking	<i>Nano Lett.</i> , 2016, 16 (10), 6425–6430; <i>Nano Lett.</i> , 2015, 15 (3), 1603–1608; <i>Nano Lett.</i> , 2016, 16 (2), 1415–1420; <i>ACS Nano</i> , 2016, 10 (2), 2485–2490; <i>Nano Lett.</i> , 2015, 15 (7), 4644–4649; <i>ACS Nano</i> , 2015, 9, 10386–10393
tetrahertz conductivity	<i>Nano Lett.</i> , 2016, 16 (8), 4838–4848
applications in optoelectronics and beyond	
LED	<i>Nano Lett.</i> , 2016, 16 (2), 1415–1420; <i>ACS Nano</i> , 2017, 11 (3), 3119–3134; <i>ACS Nano</i> , 2016, 10 (10), 9720–9729
luminescent converter	<i>ACS Energy Lett.</i> , 2017, 2, 1479–1486
photocatalytic CO <sub>2</sub> reduction	<i>J. Am. Chem. Soc.</i> , 2017, 139 (16), 5660–5663

investigation.<sup>6</sup> For perovskites, this is essential to stabilizing desirable phases and to controlling the metal-halide stoichiometry, which plays a critical role in determining the optoelectronic performance of these materials.

The first report of perovskite nanocrystals focused on CH<sub>3</sub>NH<sub>3</sub>PbBr<sub>3</sub> rather than the more commonly explored CH<sub>3</sub>NH<sub>3</sub>PbI<sub>3</sub> because of its higher stability.<sup>7</sup> In this work, Schmidt et al. synthesized 6 nm CH<sub>3</sub>NH<sub>3</sub>PbBr<sub>3</sub> nanocrystals, which could be kept stable in the solid state as well as in concentrated colloidal solutions for more than 3 months. This general synthetic approach has since been extended to CsPbX<sub>3</sub> (X = Cl, Br, or I),<sup>5</sup> CH<sub>3</sub>NH<sub>3</sub>PbX<sub>3</sub>,<sup>8</sup> CH(NH<sub>2</sub>)<sub>2</sub>PbX<sub>3</sub>,<sup>9</sup> and lead-free CsSnX<sub>3</sub><sup>10</sup> and Cs<sub>2</sub>AgBiX<sub>6</sub><sup>11</sup> perovskite compounds. The

**Published:** May 9, 2018

sizes and, therefore, quantum confinement of all of these materials could be tuned by careful control of the reaction conditions. Furthermore, a microfluidic reactor has been demonstrated to rapidly screen reaction conditions to produce perovskite nanocrystals with desired properties.<sup>12</sup> Once optimized, these conditions were also transferable to batch reactions.

Beyond direct synthesis, desired materials can also be obtained through post-synthetic reactions, such as anion exchange, cation exchange, and phase transformation. Nedelcu et al. reported intentionally partial and complete anion exchange in CsPbX<sub>3</sub> nanocrystals.<sup>13</sup> The source of the foreign ions for the exchange could be either a halide precursor or, surprisingly, other CsPbX<sub>3</sub> nanocrystals. The authors propose that this unusual exchange occurs because of the slight solubility of the halide anions in the solvent that allows dynamic dissolution and re-precipitation. As expected, this exchange process occurs over 10–20 min rather than the 30–60 s for the direct exchange. By adjustment of the halide ratios, photoluminescence could be tuned over the entire visible spectrum (410–700 nm) and the high quantum yields (20–80%) maintained, indicating a lack of optically active defects resulting from the exchange. This is in contrast to the purification that is required to achieve high quantum yields in other cation-exchanged semiconductor nanocrystals.<sup>14</sup> The high speed of anion exchange is likely a combined result of the ionic properties of the perovskite and low activation energy for the formation and diffusion of halide vacancies.

In contrast, cation exchange is more challenging and much slower in perovskites, perhaps because of high activation energies for the formation of cation vacancies or for interstitial diffusion.<sup>15</sup> Early attempts led to the decomposition of the parent nanocrystals.<sup>13</sup> Nevertheless, van der Stam et al. demonstrated the incorporation of divalent cations ( $M = \text{Sn}^{2+}$ ,  $\text{Cd}^{2+}$ , and  $\text{Zn}^{2+}$ ) into CsPbBr<sub>3</sub> nanocrystals, yielding CsPb<sub>1-x</sub>M<sub>x</sub>Br<sub>3</sub> nanocrystals with their original shape but blue-shifted band gaps.<sup>15</sup> Both anion- and cation-exchange reactions provide new possibilities by which to tune the properties of halide perovskites.

In addition to ion-exchange reactions, phase transformations offer yet another approach to tailoring the synthesis of perovskite nanocrystals. For example, Cs<sub>4</sub>PbBr<sub>6</sub> nanocrystals, called “0D” because their metal-halide octahedra do not form an extended network, are non-emissive. By reacting them with PbBr<sub>2</sub>, they can be transformed into green-fluorescent nanocrystals of the “3D” perovskite CsPbBr<sub>3</sub>.<sup>16</sup> Furthermore, as has been seen in other semiconductors, the high surface-to-volume ratio of perovskite nanostructures can stabilize unconventional phases. In contrast to the thin film and bulk crystalline form of CH(NH<sub>2</sub>)<sub>2</sub>PbI<sub>3</sub>, which is a yellow nonperovskite phase at room temperature, nanosized CH(NH<sub>2</sub>)<sub>2</sub>PbI<sub>3</sub> takes the black perovskite phase.<sup>17</sup> This black phase is photoactive and has a smaller band gap and is therefore more appropriate for solar cells and photodetectors. Given that slight distortions of the perovskite crystal structure can have far-reaching consequences in the material’s optoelectronic properties, tuning the phase of halide perovskites via nanostructuring could lead to new properties that were not achievable in bulk crystals or thin films.

Lastly, perovskite nanocrystals can be doped with foreign ions to generate new properties. One recent example comes from doping with magnetic Mn<sup>2+</sup>.<sup>18,19</sup> Bright (16–58% quantum yield) luminescence from the Mn<sup>2+</sup> defect and clear electron paramagnetic resonance spectra were observed,

confirming the presence of the impurity within the nanocrystals. This initial report of modifying the emission of the nanocrystals through doping with a magnetic impurity opens up possibilities for future magneto-optical applications.

From a synthetic perspective, halide perovskite nanocrystals offer a dizzying array of possibilities and, therefore, highly tunable properties. Beyond mixing their cations and anions, size control modifies the properties of the nanocrystals either through quantum confinement or by stabilizing unconventional phases. The controlled synthesis of nanocrystals facilitates rapid development of compositions tailored for specific applications. Finally, uniform incorporation of dopants can add new functionality to these already-versatile new materials.

### Bright, Tunable Emission and Blinking Dynamics.

Characterizing the properties of perovskite nanocrystals is essential to determining their advantages over existing materials to find appropriate applications. The most-prominent property of perovskite nanocrystals is their tunable absorption and emission. Like their bulk counterparts, perovskite nanocrystals exhibit strong absorption at energies larger than their band gap. In addition, they show strong emission in the visible region of the spectrum, from 410 to 700 nm for CsPbX<sub>3</sub>,<sup>5,12</sup> and 415 to 740 nm for CH(NH<sub>2</sub>)<sub>2</sub>PbX<sub>3</sub>.<sup>17</sup> Sn-based perovskite nanocrystals shift this range into the infrared between 500 and 950 nm,<sup>10</sup> further expanding the potential applications for these materials. Substitution and mixing of the cations and halides tunes the wavelengths of their absorption and luminescence in a broad range, while quantum confinement is used to make more-narrow adjustments. Their photoluminescence is quite narrow-band, with full width at half-maximum values of 12–40 nm (89–106 meV)<sup>5,12</sup> for inorganics and 20–44 nm (148–87 meV) for CH(NH<sub>2</sub>)<sub>2</sub>PbX<sub>3</sub>.<sup>17</sup> Photoluminescence quantum yields (PLQYs) can be remarkably high, ranging from 45 to 92% for inorganics<sup>5,6,10,12</sup> and 1 to 92% for CH(NH<sub>2</sub>)<sub>2</sub>PbX<sub>3</sub>,<sup>6,17</sup> for which the highest yield is in the green. No emission from trap states has been reported. The surface of perovskite nanocrystals is generally well passivated by the ligands used in their synthesis, although the benefits of surface modifications have yet to be fully explored. These properties are remarkable in comparison to those of chalcogenide quantum dots, which typically require core–shell structures to achieve such high PLQY values and often show emission from interband defect states.<sup>5,20</sup> Furthermore, the radiative recombination rate in perovskite nanocrystals is about 20 times faster at room temperature than that of previously studied nanocrystals because the lowest-energy excitation is an allowed transition.<sup>3</sup> Lastly, in addition to these linear properties, significant multiphoton absorption cross-sections have also been reported in CsPbBr<sub>3</sub> nanocrystals, and films of these nanocrystals display multiphoton stimulated emissions.<sup>21</sup> These absorption and emission characteristics make halide perovskite nanocrystals attractive for photophysical studies and optoelectronic applications.

High PLQY values have spurred investigation into the charge-carrier dynamics of perovskite nanocrystals. Like other colloidal nanocrystals, hybrid<sup>22</sup> and all-inorganic<sup>23,24</sup> perovskite nanocrystals and also perovskite nanocrystalline films<sup>25</sup> exhibit intermittency in their fluorescence, known as “blinking.” Blinking is undesirable from a technological standpoint because it deactivates the quantum dot unpredictably. Blinking occurs when additional charge, or charge separation of an exciton, modifies the nanocrystal’s recombination rates. This new “off” state temporarily favors nonradiative recombination rather than

radiative decay. When the charge is neutralized or the exciton decays, the nanocrystal returns to its intrinsic “on” state. Ionization via Auger recombination or the charging of surface traps are two common mechanisms that produce this “off” state; consequently, studies of Auger recombination and surface effects are critical to evaluating the potential of perovskite nanocrystals as single-photon emitters. Several initial studies show that blinking in perovskite nanocrystals increases with excitation power<sup>22–24,26</sup> and is remarkably low at low excitation,<sup>23</sup> but further work is required to determine the mechanism of blinking and strategies to mitigate it. Initial ensemble measurements of Auger decay rates in CsPbI<sub>3</sub> and CsPbBr<sub>3</sub> are 5–10 times faster than in previously studied chalcogenide quantum dots,<sup>20</sup> which could pose challenges in developing devices that depend upon high carrier densities, such as light-emitting diodes and lasers. In contrast, single-particle measurements of CsPbI<sub>3</sub> nanocrystals indicate a “grey” level in between the “on” and “off” states, which suggests that the Auger recombination rate has been slowed and no longer out-competes radiative recombination.<sup>23</sup> Clearly, further research is necessary to understand the complex charge dynamics within these materials.


The next step in the development of perovskite nanocrystals is assembling them into films or extended solids. Terahertz pump–probe studies on CsPbBr<sub>3</sub> nanocrystals indicate extremely high local carrier mobilities (4500 cm<sup>2</sup> V<sup>-1</sup> s<sup>-1</sup>), which are much higher than those found in films and comparable to bulk single crystals measured by transport techniques.<sup>27</sup> This result indicates that perovskite nanocrystals are relatively insensitive to surface defects, even though they possess a large density of dangling bonds on the surface; however, because of slower charge transport between the nanocrystals, such high mobilities are not expected in films.

**Applications in Optoelectronics and Beyond.** High photoluminescence quantum yields, rapid radiative recombination, and wavelength tunability make perovskite nanocrystals highly attractive for optoelectronics. Green, blue, and red light-emitting diodes (LEDs) have been realized just by tuning the synthesis, and their external quantum efficiencies continue to increase through device optimization.<sup>28–30</sup> Beyond LEDs, a low threshold for amplified spontaneous emission makes perovskite nanocrystals potentially viable for lasing. Stimulated emission from both one- and two-photon absorption has been observed.<sup>21,31</sup> Also, the radiative lifetime for CsPbBr<sub>3</sub> perovskite nanocrystals is greatly shortened as compared to that of metal chalcogenide nanocrystals, making CsPbBr<sub>3</sub> nanocrystals attractive as single photon emitters. In photovoltaics, although thin film perovskite solar cells have achieved efficiencies of up to 22.7%, efficiencies of devices based on perovskite nanocrystals are still very low. As has been observed in chalcogenide quantum dots, this is perhaps due to the insulating ligands on the surface of the nanocrystals, which can inhibit charge transport and induce recombination. Besides acting as the active photoabsorber, perovskite nanocrystals can also function as luminescent converters in solar cells.<sup>32</sup> In addition, one recent work shows the application of CsPbBr<sub>3</sub> quantum dots for photocatalytic CO<sub>2</sub> reduction.<sup>33</sup> Although conventional metal chalcogenide nanocrystals have been widely studied for fluorescent biological imaging, the incompatibility of perovskite nanocrystals with water, stemming from their ionic nature, makes this a challenging application for them. The nanocrystal toxicity would also have to be addressed.

**Outlook.** Perovskite nanocrystals greatly broaden the portfolio of materials available for quantum dots. The challenge ahead is to continue to take full advantage of the compositions, dopants, transformations, and new phases offered by synthesis at the nanoscale. Furthermore, perovskite nanocrystals can be assembled into extended solids in LEDs or solar cells or perhaps serve as precursors for the growth of thin films.<sup>34</sup> Such synthetic strategies are particularly welcome for all-inorganic halide perovskites for which low solubility makes it challenging to form pinhole-free films via conventional deposition processes. Correlating the chemistry of these materials to their properties and using first-principles calculations to interpret these relationships can help the community understand why these materials exhibit their remarkable performance and how to develop more-stable and less-toxic materials with similar properties. Although most work so far has focused on optoelectronic applications, perovskite nanocrystals also show potential for magneto-optics, catalysis, chemical sensing, and imaging. Nevertheless, the toxicity and poor stability of these materials are challenges that must be addressed for the field to reach its full potential.

**Sarah Brittan,**<sup>†,‡</sup> Guest Editor

<sup>†</sup>Center for Nanophotonics, AMOLF, Science Park 104, Amsterdam 1098 XG, The Netherlands

**Jingshan Luo,**<sup>∞,§</sup> Guest Editor 

<sup>∞</sup>Institute of Photoelectronic Thin Film Devices and Technology, College of Electronic Information and Optical Engineering, Nankai University, Tianjin, 300071 China

<sup>§</sup>Laboratory of Photonics and Interfaces, Institute of Chemical Sciences and Engineering, École Polytechnique Fédérale de Lausanne (EPFL), Lausanne, CH-1015 Switzerland

## ■ AUTHOR INFORMATION

### ORCID

Jingshan Luo: 0000-0002-1770-7681

### Present Address

<sup>‡</sup>Electronics Science and Technology Division, U.S. Naval Research Laboratory, Washington, DC 20375, USA

### Notes

Views expressed in this editorial are those of the authors and not necessarily the views of the ACS.

## ■ REFERENCES

- (1) Kang, J.; Wang, L. W. *J. Phys. Chem. Lett.* **2017**, *8* (2), 489–493.
- (2) Swarnkar, A.; Ravi, V. K.; Nag, A. *ACS Energy Letters* **2017**, *2* (5), 1089–1098.
- (3) Becker, M. A.; Vaxenburg, R.; Nedelcu, G.; Sercel, P. C.; Shabaev, A.; Mehl, M. J.; Michopoulos, J. G.; Lambrakos, S. G.; Bernstein, N.; Lyons, J. L.; Stoferle, T.; Mahrt, R. F.; Kovalenko, M. V.; Norris, D. J.; Raino, G.; Efros, A. L. *Nature* **2018**, *553* (7687), 189–193.
- (4) Pan, A.; He, B.; Fan, X.; Liu, Z.; Urban, J. J.; Alivisatos, A. P.; He, L.; Liu, Y. *ACS Nano* **2016**, *10* (8), 7943–54.
- (5) Protesescu, L.; Yakunin, S.; Bodnarchuk, M. I.; Krieg, F.; Caputo, R.; Hendon, C. H.; Yang, R. X.; Walsh, A.; Kovalenko, M. V. *Nano Lett.* **2015**, *15* (6), 3692–6.
- (6) Imran, M.; Caligiuri, V.; Wang, M.; Goldoni, L.; Prato, M.; Krahe, R.; De Trizio, L.; Manna, L. *J. Am. Chem. Soc.* **2018**, *140* (7), 2656–2664, DOI: 10.1021/jacs.7b13477.
- (7) Schmidt, L. C.; Pertegás, A.; González-Carrero, S.; Malinkiewicz, O.; Agouram, S.; Mínguez Espallargas, G.; Bolink, H. J.; Galian, R. E.; Pérez-Prieto, J. *J. Am. Chem. Soc.* **2014**, *136* (3), 850–853.

- (8) Zhang, F.; Zhong, H.; Chen, C.; Wu, X.-g.; Hu, X.; Huang, H.; Han, J.; Zou, B.; Dong, Y. *ACS Nano* **2015**, *9* (4), 4533–4542.
- (9) Levchuk, I.; Osvet, A.; Tang, X.; Brandl, M.; Perea, J. D.; Hoegl, F.; Matt, G. J.; Hock, R.; Batentschuk, M.; Brabec, C. J. *Nano Lett.* **2017**, *17* (5), 2765–2770.
- (10) Jellicoe, T. C.; Richter, J. M.; Glass, H. F. J.; Tabachnyk, M.; Brady, R.; Dutton, S. E.; Rao, A.; Friend, R. H.; Credgington, D.; Greenham, N. C.; Böhm, M. L. *J. Am. Chem. Soc.* **2016**, *138* (9), 2941–2944.
- (11) Creutz, S. E.; Crites, E. N.; De Siena, M. C.; Gamelin, D. R. *Nano Lett.* **2018**, *18*, 1118.
- (12) Lignos, I.; Stavrakis, S.; Nedelcu, G.; Protesescu, L.; deMello, A. J.; Kovalenko, M. V. *Nano Lett.* **2016**, *16* (3), 1869–77.
- (13) Nedelcu, G.; Protesescu, L.; Yakunin, S.; Bodnarchuk, M. I.; Grotevent, M. J.; Kovalenko, M. V. *Nano Lett.* **2015**, *15* (8), 5635–5640.
- (14) Jain, P. K.; Beberwyck, B. J.; Fong, L.-K.; Polking, M. J.; Alivisatos, A. P. *Angew. Chem., Int. Ed.* **2012**, *51* (10), 2387–2390.
- (15) van der Stam, W.; Geuchies, J. J.; Altantzis, T.; van den Bos, K. H. W.; Meeldijk, J. D.; Van Aert, S.; Bals, S.; Vanmaekelbergh, D.; de Mello Donega, C. *J. Am. Chem. Soc.* **2017**, *139* (11), 4087–4097.
- (16) Akkerman, Q. A.; Park, S.; Radicchi, E.; Nunzi, F.; Mosconi, E.; De Angelis, F.; Brescia, R.; Rastogi, P.; Prato, M.; Manna, L. *Nano Lett.* **2017**, *17* (3), 1924–1930.
- (17) Levchuk, I.; Osvet, A.; Tang, X.; Brandl, M.; Perea, J. D.; Hoegl, F.; Matt, G. J.; Hock, R.; Batentschuk, M.; Brabec, C. J. *Nano Lett.* **2017**, *17* (5), 2765–2770.
- (18) Liu, W.; Lin, Q.; Li, H.; Wu, K.; Robel, I.; Pietryga, J. M.; Klimov, V. I. *J. Am. Chem. Soc.* **2016**, *138* (45), 14954–14961.
- (19) Mir, W. J.; Jagadeeswararao, M.; Das, S.; Nag, A. *ACS Energy Letters* **2017**, *2* (3), 537–543.
- (20) Makarov, N. S.; Guo, S.; Isaienko, O.; Liu, W.; Robel, I.; Klimov, V. I. *Nano Lett.* **2016**, *16* (4), 2349–62.
- (21) Wang, Y.; Li, X.; Zhao, X.; Xiao, L.; Zeng, H.; Sun, H. *Nano Lett.* **2016**, *16* (1), 448–53.
- (22) Tian, Y.; Merdasa, A.; Peter, M.; Abdellah, M.; Zheng, K.; Ponceca, C. S., Jr.; Pullerits, T.; Yartsev, A.; Sundstrom, V.; Scheblykin, I. G. *Nano Lett.* **2015**, *15* (3), 1603–8.
- (23) Hu, F.; Yin, C.; Zhang, H.; Sun, C.; Yu, W. W.; Zhang, C.; Wang, X.; Zhang, Y.; Xiao, M. *Nano Lett.* **2016**, *16*, 6425–6430.
- (24) Raino, G.; Nedelcu, G.; Protesescu, L.; Bodnarchuk, M. I.; Kovalenko, M. V.; Mahrt, R. F.; Stoferle, T. *ACS Nano* **2016**, *10* (2), 2485–90.
- (25) Wen, X.; Ho-Baillie, A.; Huang, S.; Sheng, R.; Chen, S.; Ko, H. C.; Green, M. A. *Nano Lett.* **2015**, *15* (7), 4644–9.
- (26) Park, Y.-S.; Guo, S.; Makarov, N. S.; Klimov, V. I. *ACS Nano* **2015**, *9*, 10386–10393.
- (27) Yettapu, G. R.; Talukdar, D.; Sarkar, S.; Swarnkar, A.; Nag, A.; Ghosh, P.; Mandal, P. *Nano Lett.* **2016**, *16* (8), 4838–48.
- (28) Zhang, X.; Lin, H.; Huang, H.; Reckmeier, C.; Zhang, Y.; Choy, W. C. H.; Rogach, A. L. *Nano Lett.* **2016**, *16* (2), 1415–1420.
- (29) Protesescu, L.; Yakunin, S.; Kumar, S.; Bär, J.; Bertolotti, F.; Masciocchi, N.; Guagliardi, A.; Grotevent, M.; Shorubalko, L.; Bodnarchuk, M. I.; Shih, C.-J.; Kovalenko, M. V. *ACS Nano* **2017**, *11* (3), 3119–3134.
- (30) Kumar, S.; Jagielski, J.; Yakunin, S.; Rice, P.; Chiu, Y.-C.; Wang, M.; Nedelcu, G.; Kim, Y.; Lin, S.; Santos, E. J. G.; Kovalenko, M. V.; Shih, C.-J. *ACS Nano* **2016**, *10* (10), 9720–9729.
- (31) Xu, Y.; Chen, Q.; Zhang, C.; Wang, R.; Wu, H.; Zhang, X.; Xing, G.; Yu, W. W.; Wang, X.; Zhang, Y.; Xiao, M. *J. Am. Chem. Soc.* **2016**, *138* (11), 3761–3768.
- (32) Wang, Q.; Zhang, X.; Jin, Z.; Zhang, J.; Gao, Z.; Li, Y.; Liu, S. F. *ACS Energy Letters* **2017**, *2*, 1479–1486.
- (33) Xu, Y.-F.; Yang, M.-Z.; Chen, B.-X.; Wang, X.-D.; Chen, H.-Y.; Kuang, D.-B.; Su, C.-Y. *J. Am. Chem. Soc.* **2017**, *139* (16), 5660–5663.
- (34) Dastidar, S.; Egger, D. A.; Tan, L. Z.; Cromer, S. B.; Dillon, A. D.; Liu, S.; Kronik, L.; Rappe, A. M.; Fafarman, A. T. *Nano Lett.* **2016**, *16*, 3563–3570.